2D Advection-Diffusion Equation

The goal of this investigation was to see the evolution of the solution to the following two dimensional advection-diffusion equation:

$$\frac{\partial u}{\partial t} + c_x \frac{\partial u}{\partial x} + c_y \frac{\partial u}{\partial y} = K_x \frac{\partial^2 u}{\partial x^2} + K_y \frac{\partial^2 u}{\partial y^2} \tag{1}$$

In this method, the advection and diffusion components of the equation were split and solved individually. Leap-Frog was used to iterate advection and Forward-in-Time-Centered-in-Space (FTCS) was used to model diffusion. The plots below show the results produced using these methods, first individually, and then combined. Plots which capture the solution at a particular time-step are contour plots of the entire domain ($0 \leq x, y \leq 50$ m) and diagonal slices of the solution along the lines $y = x$ and $y = 50 - x$. Also shown is the resultant maximum value of $u(x,y,t)$ on the domain and its integral $U(t)$ as functions of the number of time-steps.

$$U(t) = \int_0^{L_x} \int_0^{L_y} u(x, y, t)\, dy dx \tag{2}$$

The attached file contains the C++ code used to generate output files named “2D_field_[NUMBER].csv”, “Slice_[NUMBER].csv”, and “control_output.csv”, with the numbers indicating the time-steps at which full solutions were saved.

Beginning with Leap-Frog, the recursive equation used to progress the advection phase of the equation is as follows:

$$u_{i,j}^{n+1} = u_{i,j}^{n-1} - c_x \frac{\Delta t}{\Delta x}\left(u_{i+1,j}^{n} - u_{i-1,j}^{n}\right) - c_y \frac{\Delta t}{\Delta y}\left(u_{i,j+1}^{n} - u_{i,j-1}^{n}\right) \tag{3}$$

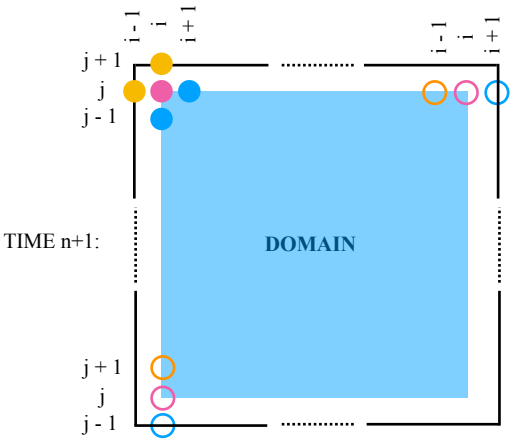

The above equation was used to advance the interior nodes of the solution. As each node is calculated using a five-point stencil, the nodes along the four boundaries of the domain were accounted for using ghost nodes — an additional row or column of nodes surrounding the domain on all four sides as shown in the diagram on the left. As illustrated, the values of these ghost nodes were assigned such that the periodic boundary condition on all four boundaries was satisfied. This method of using ghost nodes was repeated for all iterations concerning boundary nodes when solving for diffusion as well.

As Leap-Frog requires knowledge of the solutions at time *n* and *n-1* in order to calculate the solution at time *n+1*, the first iteration for advection was solved for using the Forward-in-Time-Backward-in-Space (FTBS) method with the following recursive formula:

$$u_{i,j}^{n+1} = u_{i,j}^{n} - c_x \frac{\Delta t}{\Delta x}\left(u_{i,j}^{n} - u_{i-1,j}^{n}\right) - c_y \frac{\Delta t}{\Delta y}\left(u_{i,j}^{n} - u_{i,j-1}^{n}\right) \tag{4}$$

Diffusion was calculated using FTCS:

$$u_{i,j}^{n+1} = u_{i,j}^{n-1} + K_x \frac{2\Delta t}{(\Delta x)^2}\left(u_{i+1,j}^{n-1} - 2u_{i,j}^{n-1} + u_{i-1,j}^{n-1}\right) + K_y \frac{2\Delta t}{(\Delta y)^2}\left(u_{i,j+1}^{n-1} - 2u_{i,j}^{n-1} + u_{i,j-1}^{n-1}\right) \tag{5}$$

FTCS is an implicit scheme for diffusion. A stable treatment of diffusion can stabilize advection but not vice versa. For this reason, even though FTCS is unconditionally unstable for advection, it was still an appropriate choice to solve a 2D advection-diffusion equation. We can define the Von Neumann number, s, which relates the time step, Δt, to the grid size, Δx (if we look at a one-dimension case) when we observe diffusion with a constant diffusivity of K.

$$s \equiv K \frac{\Delta t}{\Delta x^2} \tag{6}$$

What this means is that there is a high computational cost of grid refinement. A stability analysis allows us to conclude that FTCS is conditionally stable when $s \leq ½$. In two dimensions, this means that our restriction is:

$$K_x \frac{\Delta t}{\Delta x^2} + K_y \frac{\Delta t}{\Delta y^2} \leq \frac{1}{2} \tag{7}$$

As there can be instances when $\lambda < 0$ if $s > ¼$, in practice we use $s \leq ¼$. When coupled with advection, a scheme to solve the 2D advection-diffusion equation is stable when there is "enough diffusion". This can be determined using the grid Péclet number, which is a ratio of advection and diffusion in terms of Δx.

$$Pe_g \equiv \frac{c \Delta x}{K} \tag{8}$$

This value should be less than 2. If we were to use only FTCS to model the advection-diffusion, then we would need to increase K by adding artificial diffusion to make the solution better. However, by using operator splitting and modelling advection using Leap-Frog, a scheme which is conditionally stable for advection, we can achieve the following results. Using the above restrictions, I ran experiments 1 to 3 with $\Delta t = 0.1$ seconds. This ensured that $s \leq ¼$. From past analyses we know that stability of Leap-Frog depends on Courant's number, C. In particular, we want $|C| \leq 1$ or, more accurately, we want:

$$\left(c_x \frac{\Delta t}{\Delta x} + c_y \frac{\Delta t}{\Delta y} \right)^2 \leq 1 \tag{9}$$

Choosing $\Delta t = 0.1$ seconds ensured that this condition was also satisfied. For consistency and better comparison, $\Delta t = 0.1$ seconds was used for all experiments, 1, 2, and 3.

Experiment #1 models just advection using Leap-Frog.

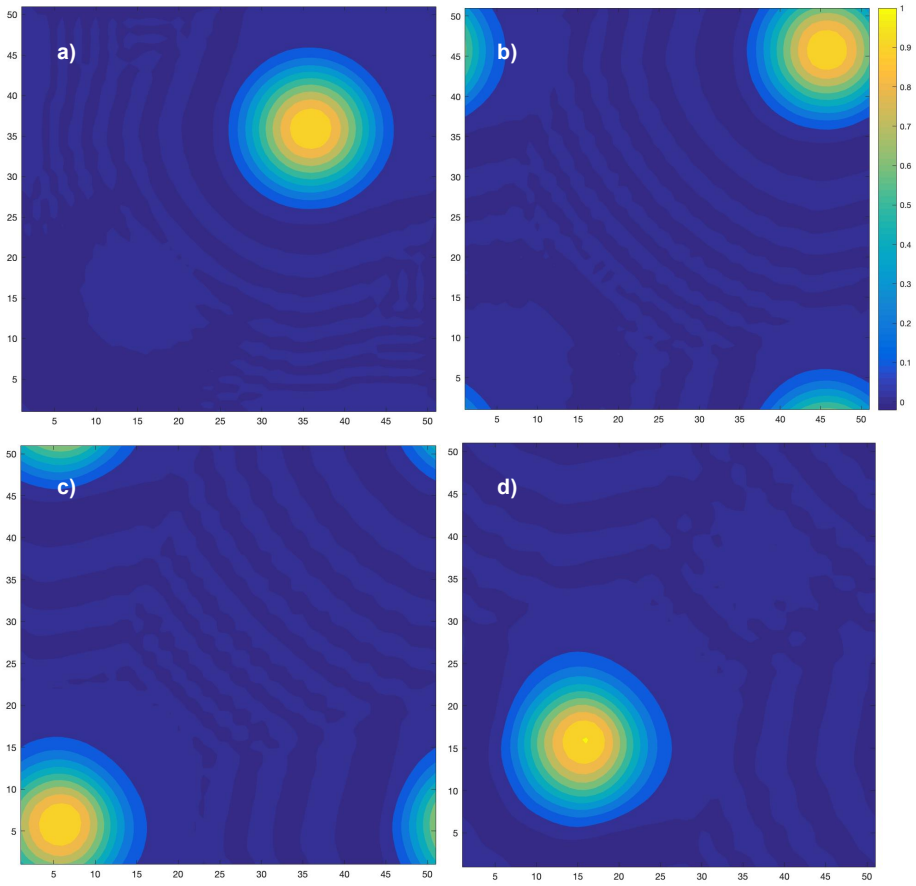

Figure 1A is a series of contour plots showing the physical solutions every 10 seconds beginning at 10 seconds. From (a) to (d) we can see that the dome moves in a northeastward direction as wave propagation speed is 1.0 m/s in both the x and the y directions. This means that it takes 50 seconds for the solution to reach its initial position, as predicted and shown here.

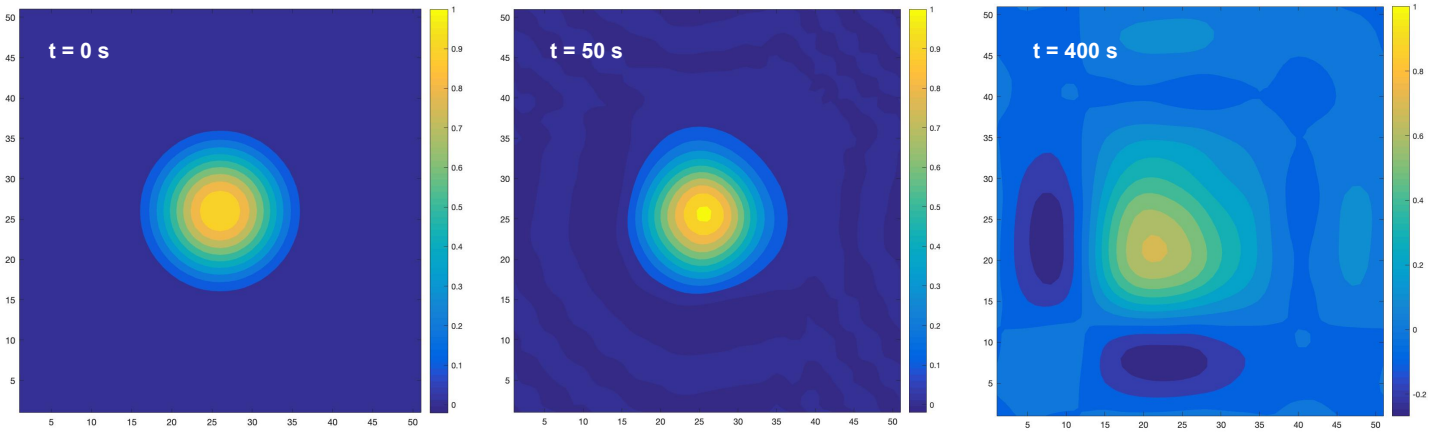

Even though there is no diffusion, there exists some deformation of the dome or bubble. Above is a contour plot of the solution at 50 seconds and another at 400 seconds.

In all the previous solutions, we see a series of patches of negative values of *u(x,y)* which seem to trail behind the dome. After 400 seconds, we see that these patches in the dome's wake are negative to a larger

degree and seem to interact with the positive values such that there is a steep gradient from negative to positive directly south and west of the bubble. These negative values are caused by computational modes that inherently exist in the scheme. These interactions show that it is likely that the computational modes of previous time-steps are compounded, causing an increase in the degree of negativity and the effect on the solution as, with the absence of diffusion, we would expect the shape of the bubble to remain perfectly spherical as in the initial condition. It is also important to clarify here that while the bubble is propagating towards the northeastern corner, we begin to see two peripheral bubbles on the northwestern and southeastern corners of the domain as well. This is due to the periodic nature of the boundary conditions which can be interpreted using the diagram below. The appearance of these peripheral bubbles is also discussed alongside Figure 1C.

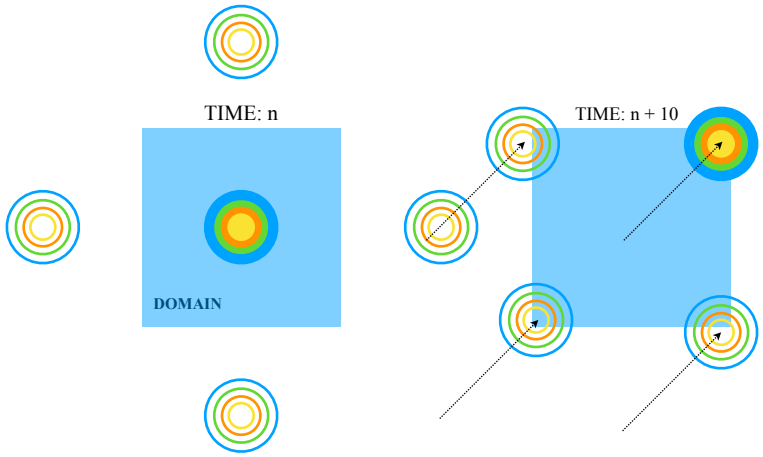

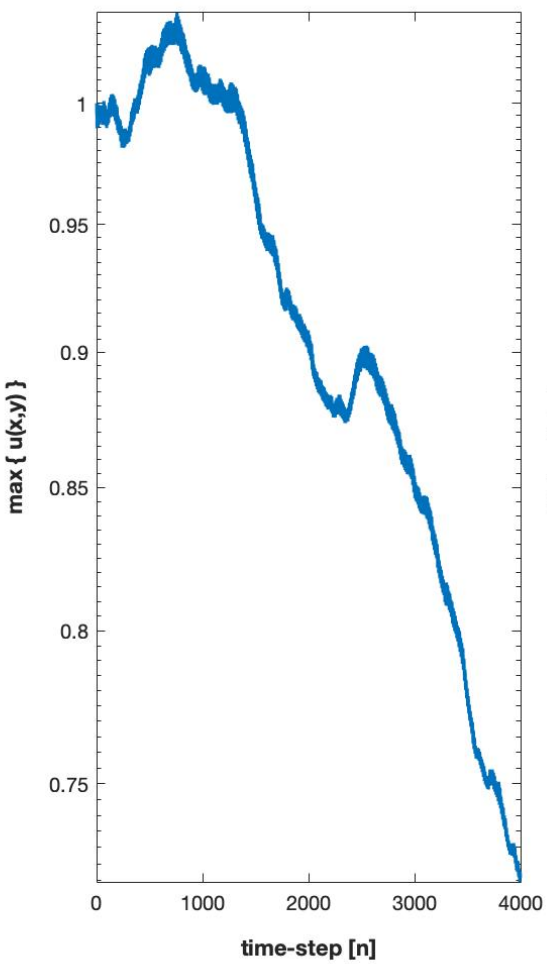

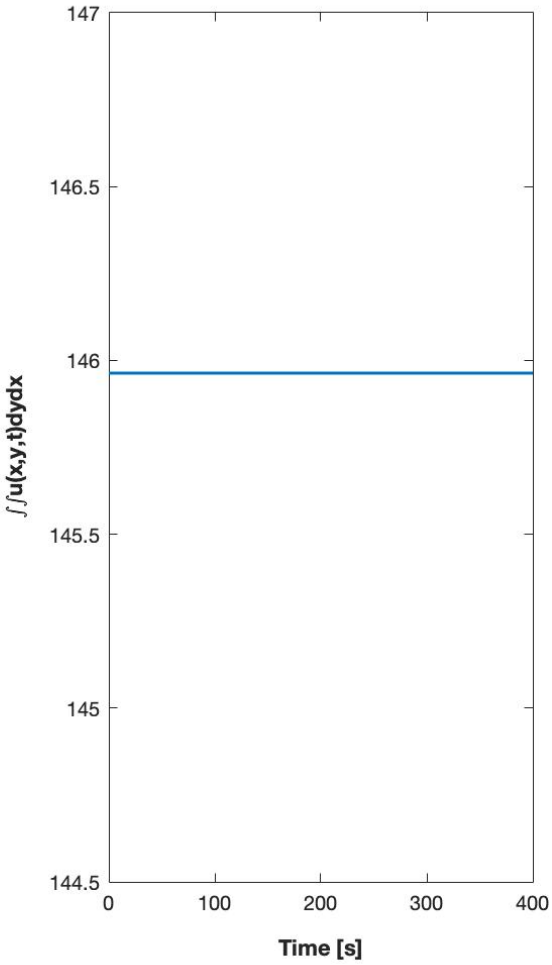

Figure 1B can be used to gauge the stability and consistency of Leap-Frog as a scheme to solve for 2D advection. The plot above shows that the maximum value of *u(x,y)* on the domain decreases with time as the solution advances. This is difficult to explain as, in the absence of diffusion, we expect the shape of the bubble to remain intact. The previous analysis shows that this was not the case. This inconsistency could be due to the presence and compounding interaction of computation modes; however, as we expect the computational mode to oscillate, the decreasing trend in amplitude remains largely unexplained. On the other hand, the plot of the integral of the domain as a function of time suggests that Leap-Frog is, in fact, consistent as the integral is conserved. This means that the increasing degree of negative patches which evolve in the solution are proportional to the increasing spatial size of the dome, allowing the integral to be maintained.

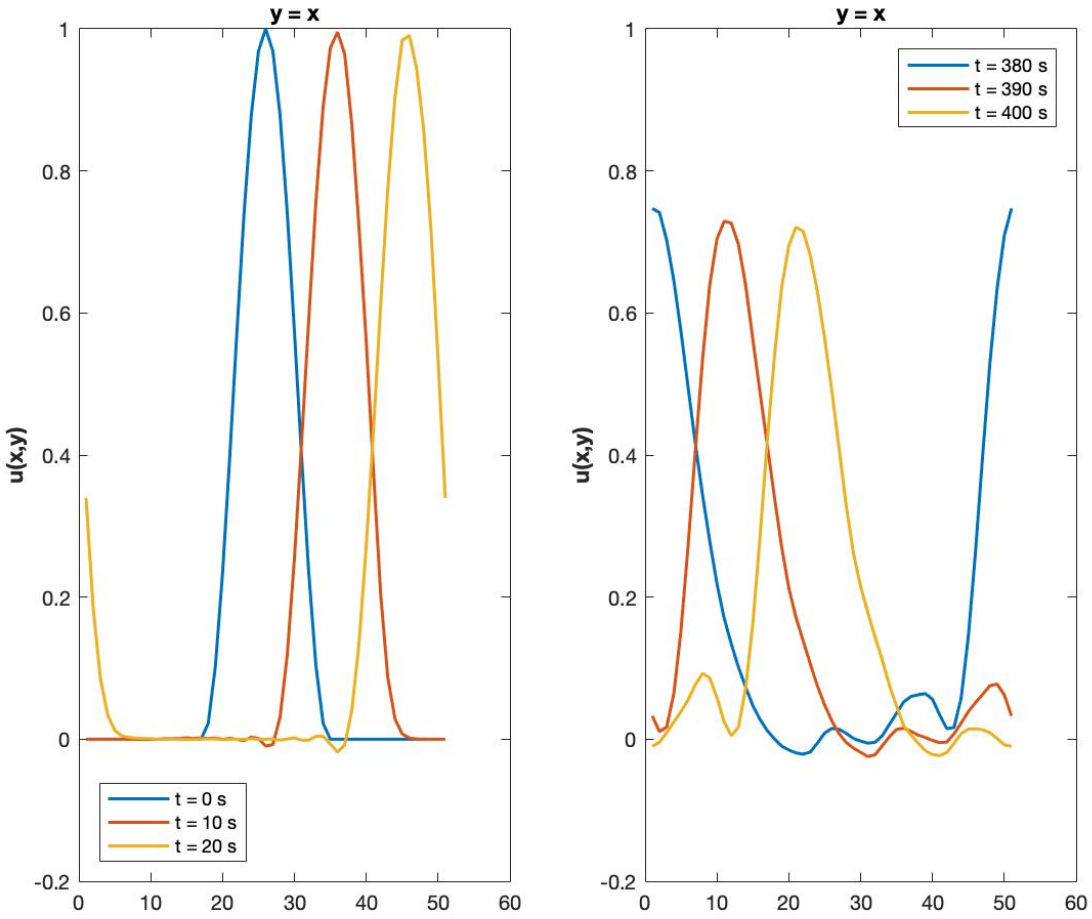

Figure 1C shows decreasing height of the bubble as viewed along the line y = x that diagonally bisects the domain. We can also see the deepening wake behind the wave which leads to the formation of smaller, secondary waves which trail behind the dome. Perhaps the decrease in amplitude is due to the formation of these waves. To conserve the integral, the height of the main wave must decrease in order to allow these smaller waves in its wake to grow. I presume that when the maximum heights are summed, the total height of main wave and of the smaller trailing waves will be much closer to the original amplitude of 1. We can also see that as time progresses, the waves which start symmetrical become increasingly right skewed. This is consistent with how the shape of the dome changes. As we recall from the 2D contour plot, there exist steep gradients on the southern and western sides of the dome whereas the northern and the eastern sides are more gently sloping.

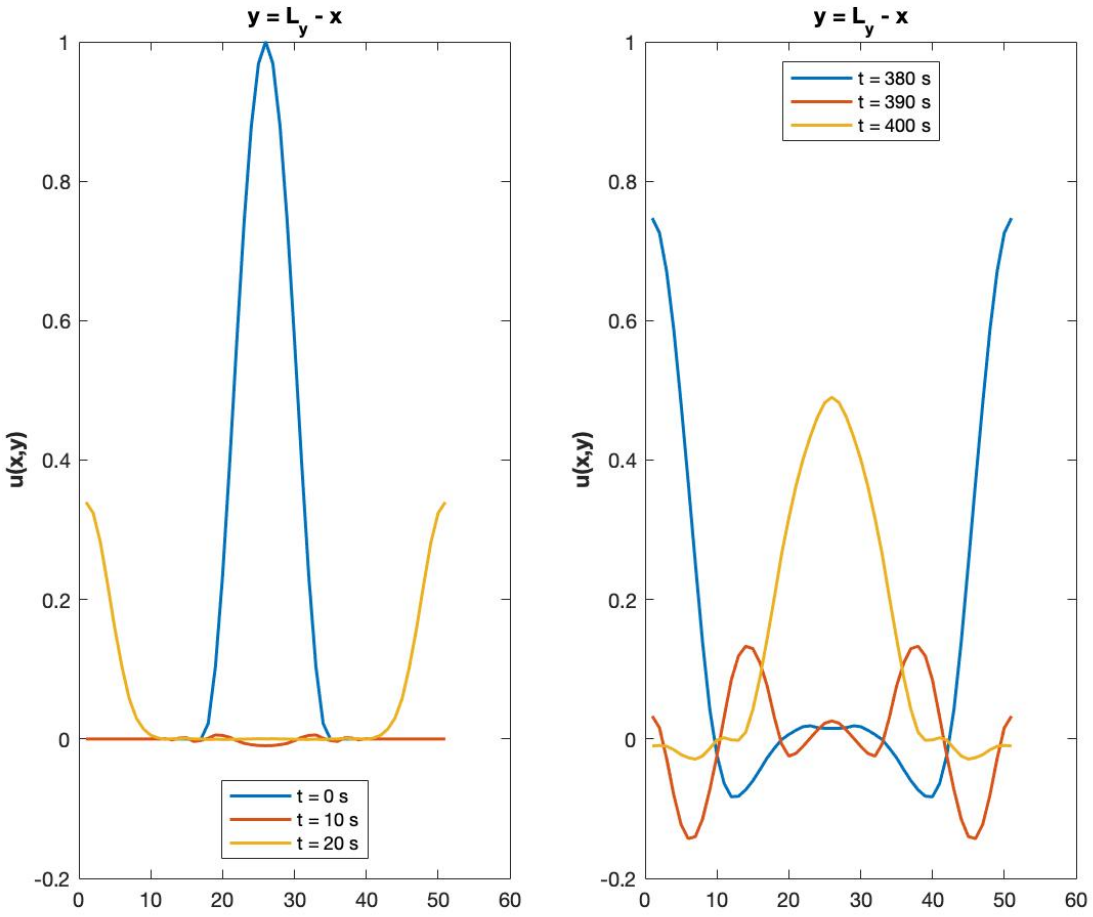

The alternative diagonal shows us another perspective. We see that the bubble starts as a perfectly symmetrical dome. In 10 seconds, it propagates far enough from the line y = 50 - x to not be visible along the slice of this diagonal. After this, the peripheral bubbles, appear on the two ends of the slice. Looking at the last three time steps, the smaller amplitude of the dome is once again clear. From this slice, the dome remains symmetrical along both sides of the peak. We can also see the wake of negative values trailing on either side of the main dome and the peripheral domes. As the dome spreads in its spatial size over time, it becomes slightly more visible even when it moves away from the line y = 50 - x. This is shown by the little peaks that still exist.

Another point to note is that FTBS waves are dampened. The smaller the Δt, the more pronounced the dampening effect as FTBS has a leading order error $\mathcal{O}(\Delta t^2, \Delta x^2)$. This is because the smaller the Δt, the smaller the Courant's number, C, and the greater the artificial diffusion that is manifested in the calculations. Leap-Frog itself has a leading order error term of $\mathcal{O}(\Delta x^2)$ so the error is not diffusivity related but perhaps it is carried forward from FTBS and perpetuated as the solution evolves. An improvement to the solution would be to decrease grid size and therefore decrease Δx.

Experiment #2 is an analysis of FTCS as a model for diffusion.

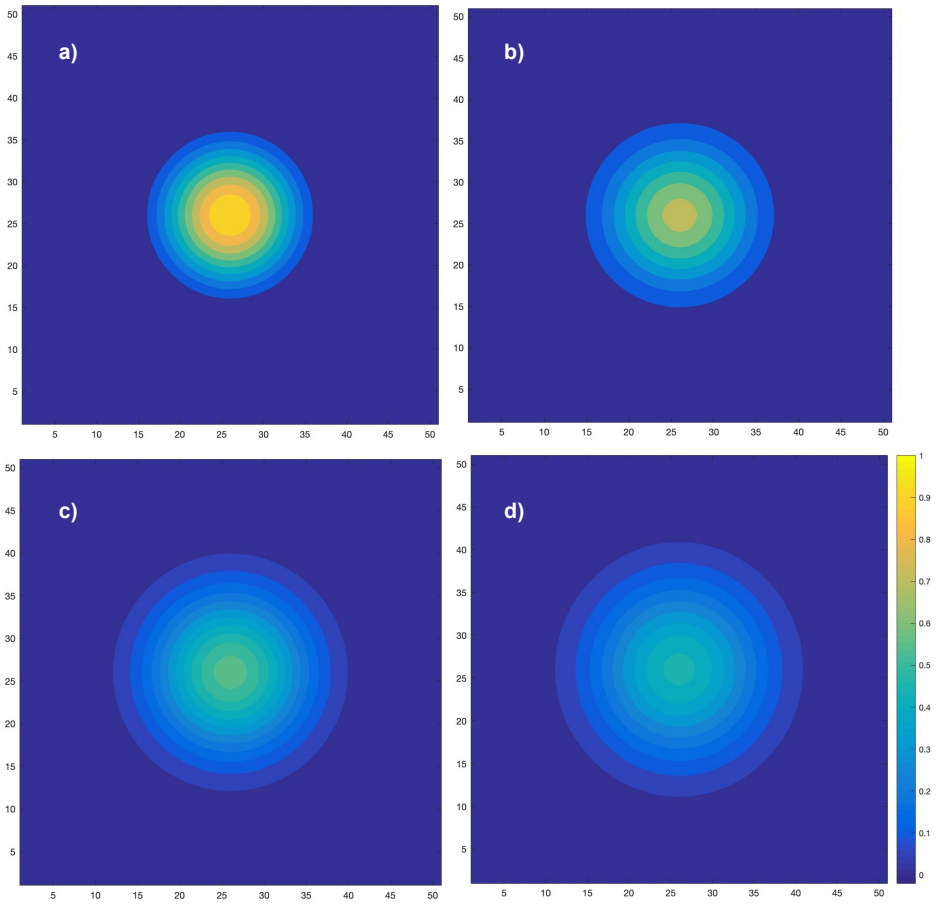

Figure 2A shows the progression of the solution every 10 seconds beginning from the initial solution. As the size of the dome increases, the height decreases. From all angles, this change is symmetrically observed, as one would expect with diffusion in the absence of advection.

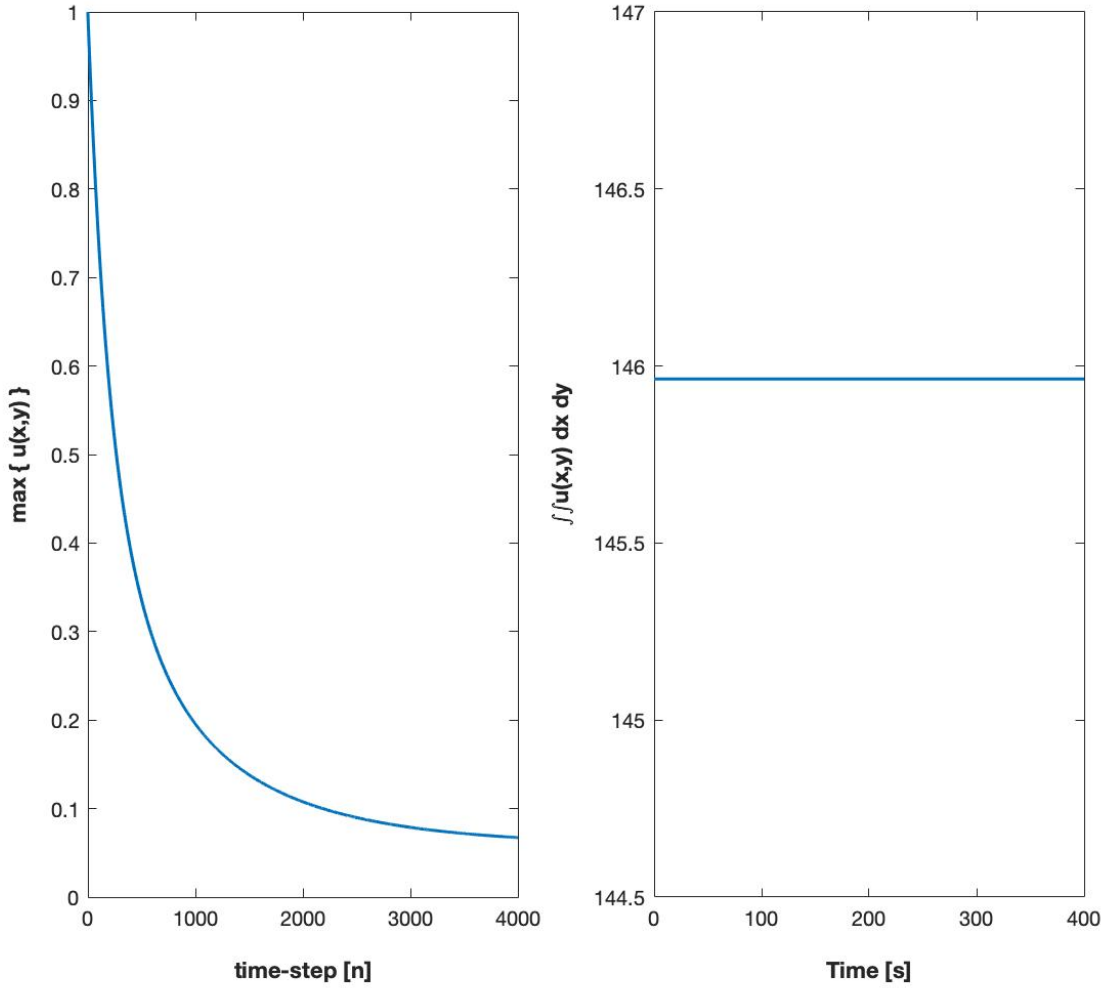

Figure 2B indicates that the maximum value of *u(x,y)* on the domain decreases smoothly with time. The rate of decrease is greatest at the beginning, followed by a slow plateau by the time the solution completes 8 cycles. This is as we expect. This is because diffusion is slowed as the gradient decreases. The conservation of the integral over the domain shows that FTCS is a stable scheme for approximating diffusion.

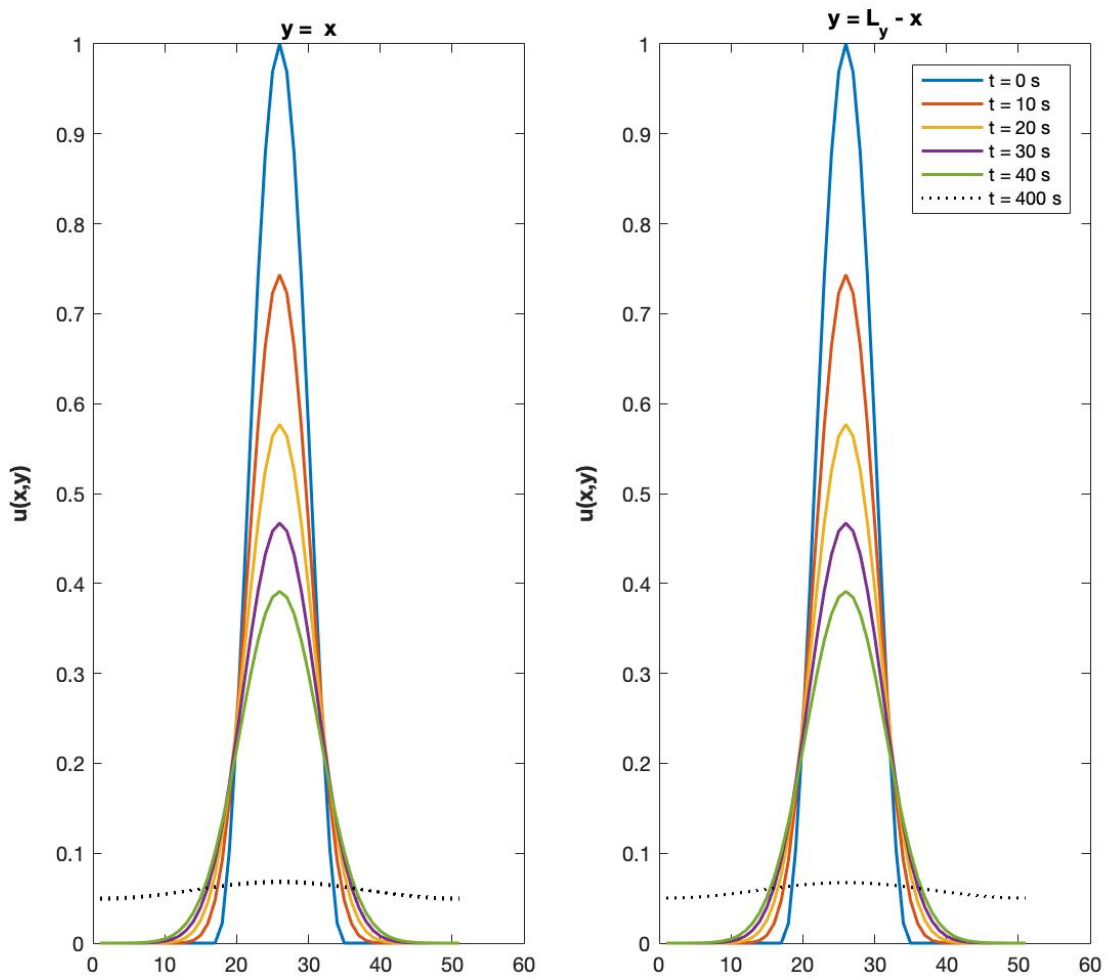

Figure 2C shows that this symmetric diffusion is preserved throughout. By the time we are on the 4000th time-step, the plot of *u(x,y)*, as visualized from the diagonal slices, is almost uniform across the domain. To maintain the integral we have larger values observed at the edges and smaller values in the middle when compared to the original solution.

In sum, FTCS very perfectly represented diffusion for this experiment. This is because our stability condition for FTCS requires that $|\lambda| \leq 1$ where $\lambda = 1 + 2s(\cos(k\Delta x) - 1)$. Another point to note is that FTCS has leading order error of $\mathcal{O}(\Delta t^2, \Delta x^4)$. As the solution behaves as it should, we can assume that the choice of Δt and Δx are sufficient.

Experiment #3 combined advection and diffusion to see the effect of both on the domain. Contour plots showing the physical solutions every 20 seconds are shown below (**Figure 3A**).

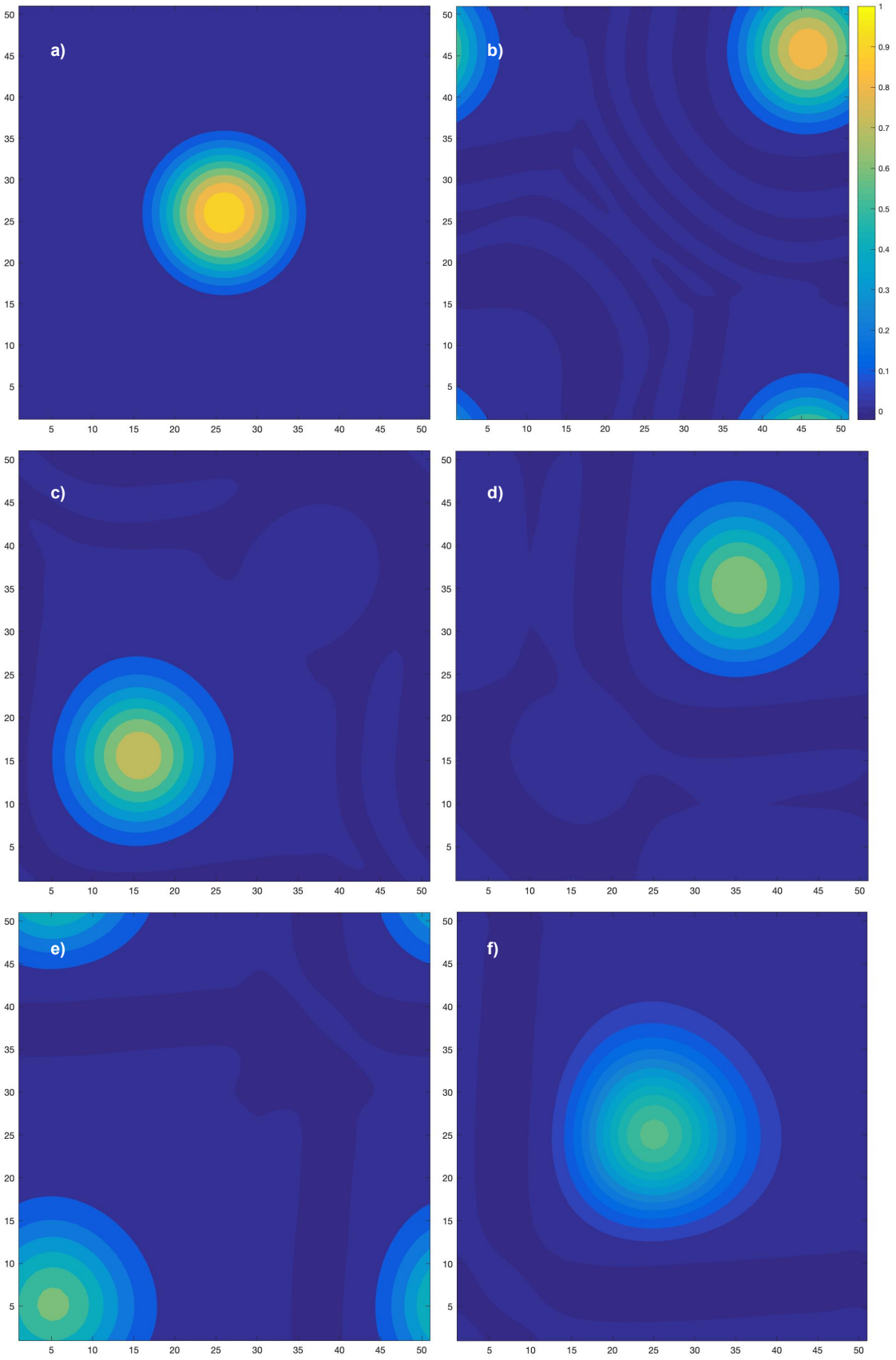

The solution passes through its initial position exactly twice within 100 seconds which is consistent with the phase speed of the advection. The effect of diffusion is also clear — the highest peak is observed in (a), the initial solution. As we progress through time from (a) to (f), the peak becomes progressively lower in height and the dome spreads in diameter accordingly. Another interesting observation is the appearance of certain negative values of *u(x,y)* which are caused by the computational modes which were discussed earlier.

We can plot the maximum value of *u(x,y)* at a given time to visualize how diffusion acts on the height of the dome.

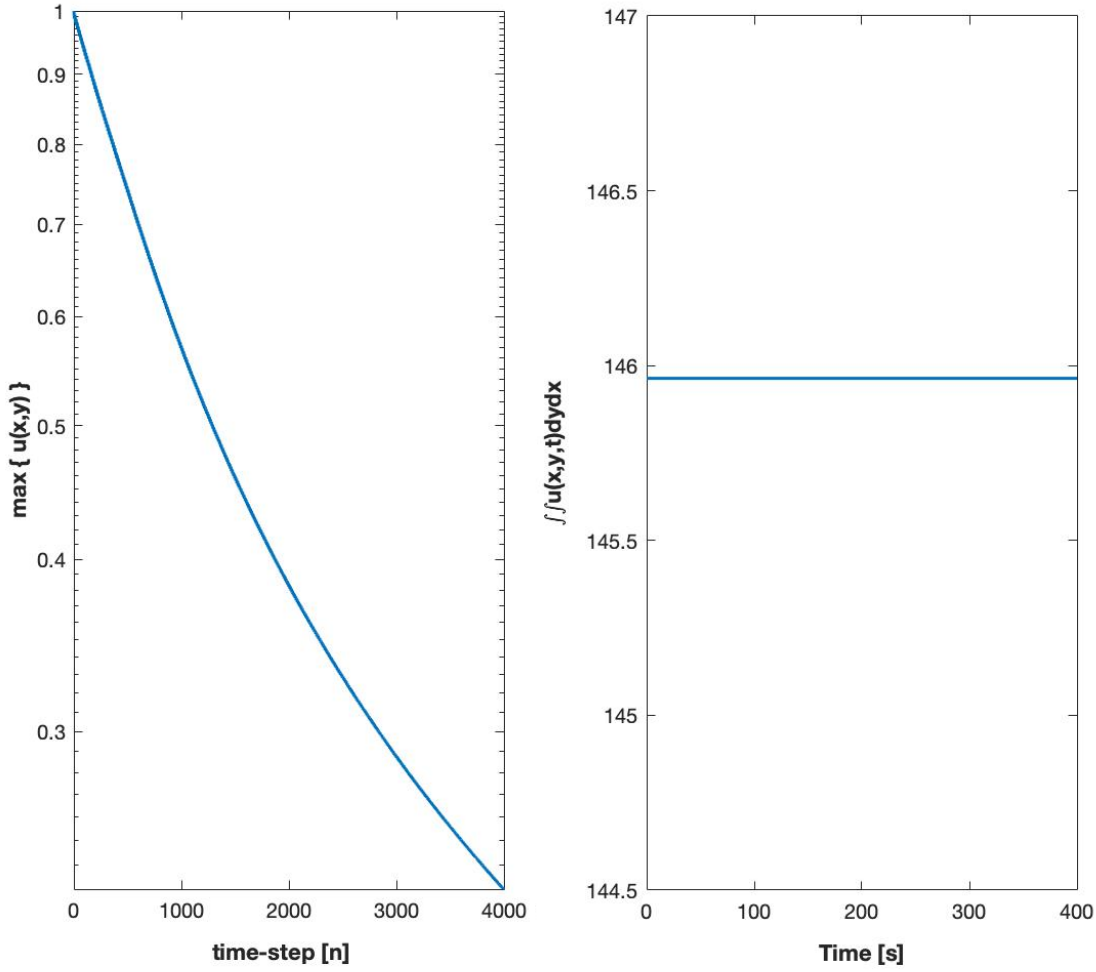

Figure 3B shows that within a period of 4000 time-steps, the maximum height decreased from 1 to around 0.2. The decrease during the first 1500 time-steps was the steepest, as expected. Due to conservation of *u(x,y)* on the domain, we expect the maximum to converge to a value which will be uniform across the grid. The integral of *u(x,y)* can be used to analyze the stability and consistency of the solution. As can be seen, the value of the integral stays consistent, implying that our scheme is stable, at least for the first 400 seconds. This suggests that the choice of $\Delta t = 0.1$ seconds was appropriate.

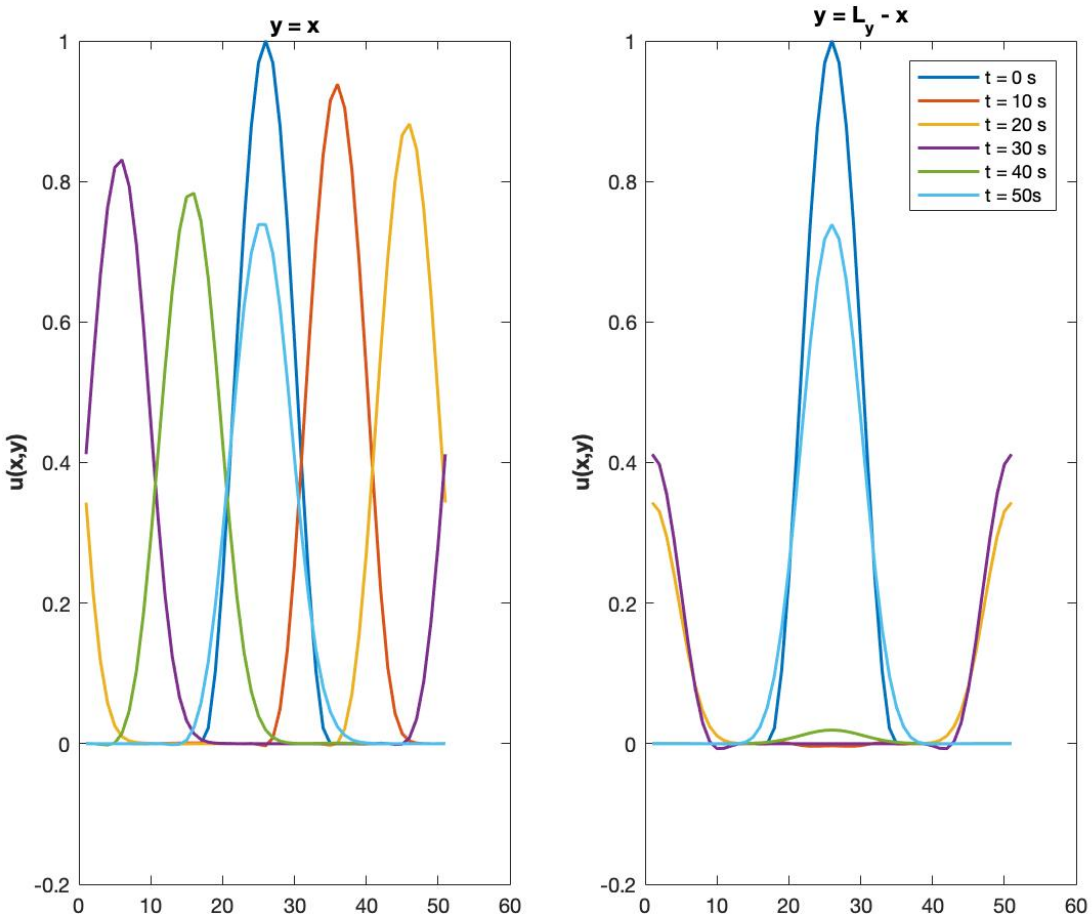

Figure 3C captures the solution along the diagonals of the domain. Along y = x, we can clearly see a decreasing height of the bubble and a widening base of the solution. The slight tendency of the wave to become right skewed is also evident when comparing the slices at the initial time and at 50 seconds. This observation was discussed in a little more detail in Figure 1C. Along the other diagonal, we can visualise the diffusivity more clearly. The widening base of the solution and the shortening height is comparable every 50 seconds.

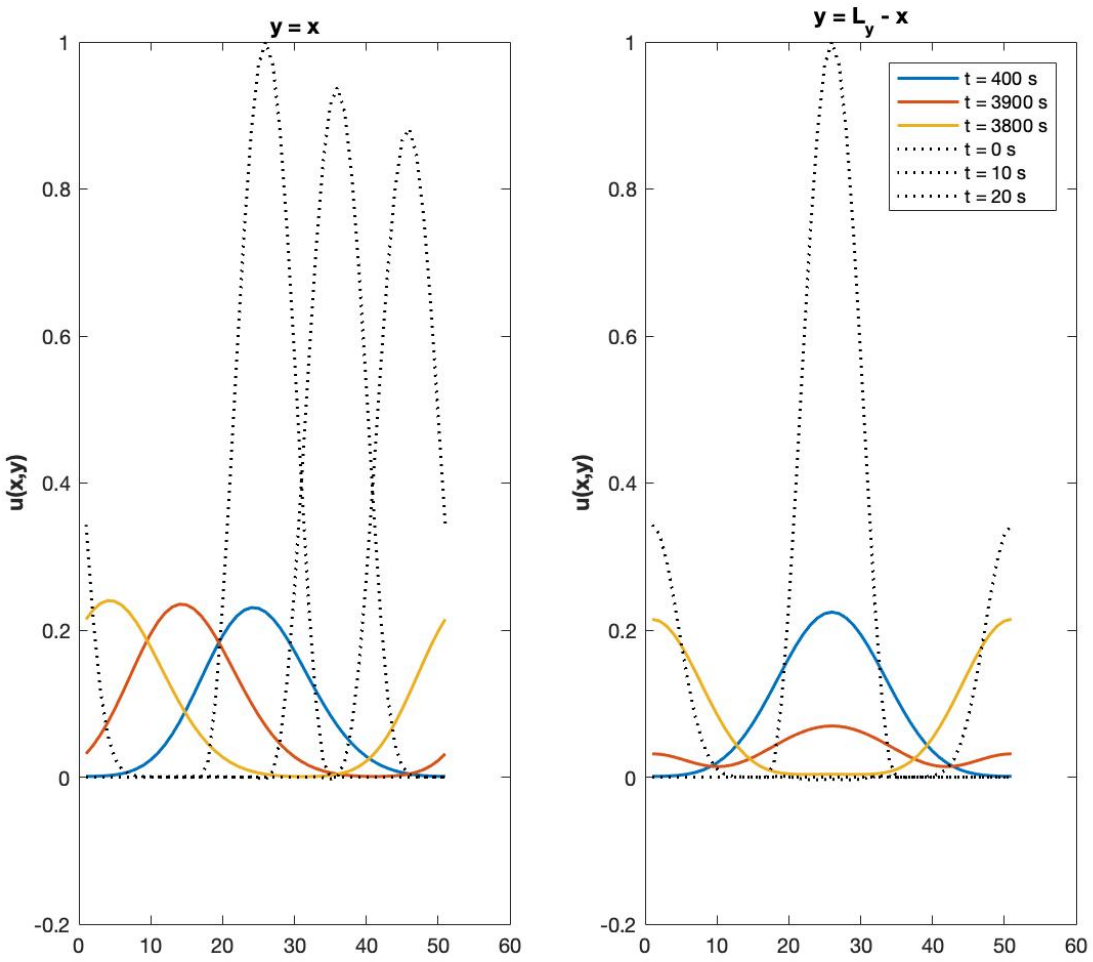

Letting the simulation run for 400 seconds (8 complete cycles), we can compare the rate of decrease of the height of the dome during the first 20 seconds to that which occurs during the last 20 seconds. As expected and discussed previously, the rate of decrease in height is greater initially and plateaus as time progresses. The right skewed nature of the solution is also less pronounced compared to the advection only case. This is likely due to the diffusion which works as a counter-measure and evens out the asymmetrical tendency of the Leap-Frog solution for advection. After 400 seconds, it looks like the peripheral bubbles and the main bubble are very similar in shape and size.

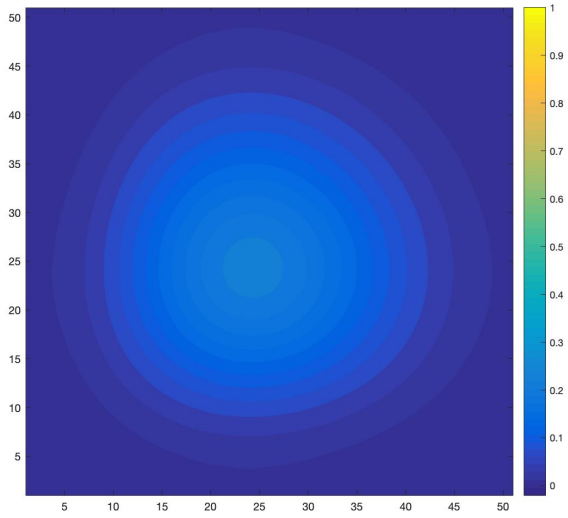

On the left is the contour plot for the solution at 400 seconds. Interestingly, there are no negative patches here which further explains why the right skew is less noticeable on the above slice along y = x. However, the solution is still not perfectly symmetrical along all sides. This suggests that diffusion using FTCS tries to maintain the symmetry of the dome while the Leap-Frog advection gives rise to computational modes in the dome's wake which cause it to stretch unevenly.

The table summarizes the Courant and Von Neumann numbers for each experiment. Grid Péclet number is also calculated and displayed although it is not relevant here as we use operator splitting instead of simply FTCS to approximate both advection and diffusion.

Recall that $C = c_x \frac{\Delta t}{\Delta x} + c_y \frac{\Delta t}{\Delta y}$ and $s = K_x \frac{\Delta t}{\Delta x^2} + K_y \frac{\Delta t}{\Delta y^2}$ and note that for diffusion we use $\Delta t = 0.2$ seconds.

Stability analyses concluded that we required $|C| \leq 1$ and $s \leq ¼$. $Pe_g = C / s$.

EXPERIMENT	**C**	**s**	**Pe_g**
#1	0.2	0	undefined
#2	0	0.2	0
#3	0.2	0.2	1